Characteristics of Non-Newtonian Fluids over Tube Banks

Er. R. P. Ram
Department of Chemical Engineering, Institute of Engineering and Technology, Lucknow-21

Abstract ***Forced convection characteristics of non-Newtonian fluids over the tube banks have been studied numerically for the following governing parameters: solid volume fractions of the cylinders; = 0.20, 0.25 and 0.30, Reynolds number; Re= 1, 5 and 10; power-law index n= 0.8, 1 and 1.4 and at a fixed value of Prandtl number of Pr=1. The flow and thermal features such as streamlines, isotherm patterns, drag coefficients and mean or average Nusselt number etc. have been explored and found to be strongly dependent over the above parameters. The drag coefficients were seen to be increased with the increasing values of solid volume fractions and power-law index, whereas, an opposite behavior was noticed with increasing Reynolds number. Further, the mean Nusselt number were found to be enhanced with increasing values of Reynolds numbers and porosity, but a decrease was noticed with increasing value of power-law index. Overall, a non-monotonous behavior has been observed for both flow and heat transfer features of non-Newtonian fluids through the tube banks.***

Index Terms: Porosity, Nusselt number, Power-law index, Drag coefficients, Cylinders

I. INTRODUCTION

The momentum and heat transfer features of fluids over tube banks are found significant in the various heat and mass transfer processes, fluidized bed drying of fibrous materials, filtration of paper and pulp suspensions etc. [1-3]. The main issue is the determination of local and global characteristics of flow and thermal parameters across the tube banks consisting arrays of cylinders in different arrangements. Previously, numerous efforts have been made to know the physical insights of different fluids and particularly non-Newtonian fluids from such an industrially important geometry. It is also pertinent to add here that a majority of the previous works are concerned with the flow and thermal characteristics of Newtonian fluids [4-7]. Conversely, low attention has been paid to the similar investigation of non-Newtonian fluids in spite of their widespread applications in food processing, autoclave process to synthesize polymer composites, filtration of polymer solutions and heating/cooling of process streams, etc. [8-12]. Furthermore, most of materials as used in the industry display a variety of rheological difficulties including shear-thickening, shear-thinning and viscoelasticity, etc. These features have been mostly investigated independently either for fluid flow [13-14] or for the heat transfer of shear-thinning fluids [15]. Overall scant studies on non-Newtonian fluids for an array of cylinders and/or over tube banks are available which are not enough to reveal the flow and heat transfer features extensively.

II. PROBLEM DESCRIPTION

The flow of power-law fluids across periodic array of circular cylinders has been considered in a square arrangement as shown in Fig. 1(a). The steady, laminar and 2-D flow is occurring in the transverse direction. It is assumed that the cylinder arrays have a large number of rows through which the fluids are flowing and therefore, the end effects are neglected. Further, the flow is repeating over the periodic geometry, and so it has also been assumed that the periodicity occurs in the vicinity of periodic boundaries. The above circular cylinders have the diameter d and tube pitches p (Fig. 1(a)), which is centre to centre distance between the cylinders. Further, the porosity of the cylinders in terms of solid volume fractions ( ) is defined in terms of tube pitches and diameter of the cylinders and is given by $= \pi/4(p/d)-2$.

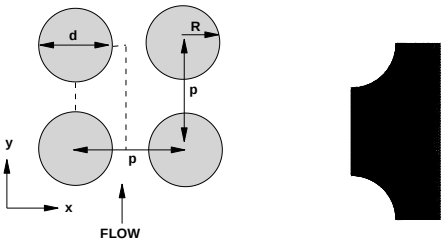

(a) (b)

Fig. 1: (a) Schematics of flow diagram and (b) computational domain

The numerical simulations have been done for half of the computational domain due to the flow and thermal symmetry conditions (Fig. 1(b)). The temperatures of flowing fluid and cylinder surfaces are maintained at T_f and T_c respectively, where $T_c > T_f$. Further, the properties of the fluids (density, viscosity, heat capacity and thermal conductivity) are assumed to be temperature independent and the viscous dissipation are also neglected.

A. Governing Equations and Boundary Conditions

In view of above assumptions and conditions, the mathematical equations for the problem defined above under the 2-D, steady and laminar flow conditions is given as follows:

Continuity Equation: $\nabla \cdot v = 0$ (1)

Momentum Equation: $\rho v \cdot \nabla v = -\nabla p + \mu \nabla^2 v$ (2)

Energy Equation: $\rho c_p \nabla . Tv = k \nabla^2 T$ (3)

Where, v is the velocity vector, ρ, c_p, μ and k are density, specific heat, viscosity and thermal conductivity, respectively.

The rheological equation of state for the power-law fluids is defined by;

$$\tau_{ij} = 2\eta\varepsilon_{ij} \qquad (i, j = x, y) \qquad (4)$$

Where, ε_{ij} is component of rate of strain tensor defined elsewhere (16) and the viscosity (η) of the non- Newtonian fluids is given by;

$$\eta = m(I_2/2)^{(n-1)/2} \qquad (5)$$

Where, n and m are the power-law indices and I_2 is known as second invariant of strain tensor [16].

The solution of above governing equations have been done by imposing the standard no-slip boundary conditions on the cylinder surfaces which are maintained at constant temperature (T_w). Further, periodically fully developed flow and temperature fields are applied across the periodic boundaries. Also, the fluid surfaces not in contact of cylinders are taken as symmetric and adiabatic. The numerical simulation of governing equations along with the boundary conditions yields velocity (V_x and V_y), pressure (p) and thermal (T) fields, which are further utilized to presume the drag [17] and the average Nusselt number as defined below;

$$Nu = \int_S Nu(\theta) d\theta \qquad (6)$$

Where, S represents the surface of cylinders exposed to the flow.

III. NUMERICAL METHODOLOGY

The governing equations along with the noted boundary conditions have been solved using the CFD solver ANSYS FLUENT. Further, an unstructured non-uniform grid consisting of triangular cells have been created by using commercial grid tool GAMBIT. A fine mesh was generated adjacent to the cylinder surfaces to resolve the sharper gradients better. A second order upwind scheme has been used to discretize the convective terms appearing in both flow and thermal equations. The double precision solver have been utilized to improve the accuracy of solutions and the results were achieved when the continuity, momentum and energy residuals reached in the order of 10^{-9} and 10^{-12}, respectively.

IV. RESULT AND DISCUSSIONS

The numerical simulations of power-law fluids have been carried out for the following pertinent dimensionless parameters: Reynolds number (Re) = 1, 5, 10; power-law index (n) = 0.8, 1, 1.4 solid volume fraction (ϕ_s) = 0.2, 0.25 and 0.30 and Pr=1. The numerical results were obtained and discussed in this section with the variations of above parameters. However, before discussing the new results, present numerical approach has been validated with the available literature as follows:

Table 1 compares the present results for drag coefficient (C_D) and average Nusselt number (Nu) with the available literature. It can be seen that the present results of drag coefficient compares well with the Vijaysri et al. [3], Soares et al. [12] and Spelt et al. [13] with the deviations of 5.90% and 2.05% at Re=1 and 40, respectively for the ϕ_s = 0.30 and n=1. Similarly, the maximum deviations in the Nu value is 3.01% with the results of Mangadoddy et al. [15]. In view of these well contrast, the present results have been generated within the range of parameters studied herein and discussed in the next sections.

Table 1: Comparison of present values of total drag coefficient (C_D) and Nusselt number with literature (ϕ_s = 0.30)

Source	n=1 (C_D)		n=1.4 (C_D)	n=1 (Nu)
	Re=1	Re=40	Re=1	Re = 1, Pr = 5
Present Results	144.7263	4.1673	202.8281	2.5295
Vijaysri et al. [3]	136.1900	-	-	-
Soares et al. [12]	136.1800	-	-	-
Spelt et al. [13]	142.1367	4.2529	205.8700	-
Mangadoddy et al. [15]	-	-	-	2.6057
δ_{max} (%)	5.90	2.05	1.50	3.01

A. Streamline Patterns and Total Drag Coefficients (C_D)

The streamline patterns are shown in Fig. 2(a) with the variations of Reynolds number (Re), power-law index (n) and solid volume fractions (ϕ_s). In Fig. 2(a), at ϕ_s =0.30 and Re=1, the curved streamlines can be seen nearer to the cylinders for all of the shear-thinning (n < 1), Newtonian (n=1) and shear-thickening (n >1) fluids (Fig. 2a). Such streamlines were appeared because of the strong interference between the two periodic cylinders at the higher value of solid volume fraction (ϕ_s =0.30). Further, the dense streamlines can be seen for shear-thinning fluids over the surface of cylinders in contrast to Newtonian and shear-thickening fluid (Fig. 2a). The impact of increased solid volume fractions are also displayed in Fig. 2(a). As the ϕ_s =0.30 decreases from ϕ_s =0.30 to 0.20, the interference between the two cylinders are getting weak, resulting, the streamlines are less curved and dense for ϕ_s =0.20 as compared to ϕ_s =0.30. The influence of increased Reynolds number can be seen with the increased fluid circulation behind the cylinder with increasing values of Reynolds number for both of the n and ϕ_s .

For instance, at Re = 10, the streamlines are observed to be denser and less swirled as compared to Re=1. The denser streamlines for Re=10 suggest that the discharges between the two consecutive streamlines are increasing with the increasing value of Reynolds Number. Next, the influences of power-law index can also be seen clearly over the streamline patterns in Fig. 2(a). As the fluid behavior changes from Newtonian to shear-thinning and shear-thickening, the density of streamlines increases and decreases, respectively for all the value of ϕ_s and Re.

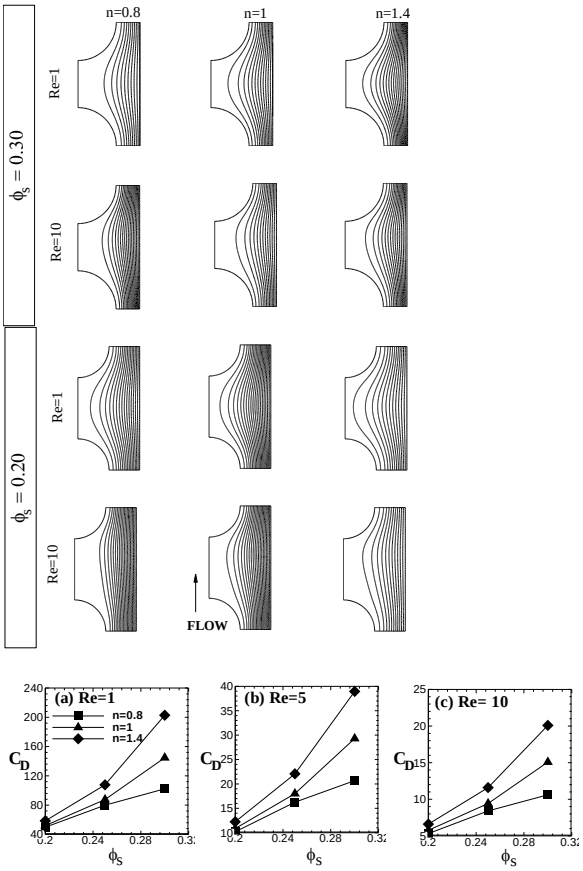

Fig. 2: (a) Streamline patterns for ϕ_s =0.30 and 0.20 and (b) Dependence of C_D on ϕ_s , Re and n

So, a stronger dependence of streamline patterns was seen for shear-thinning fluids in contrast to shear-thickening fluids Overall, the complex streamline patterns have been observed for the power-law fluids owing to shear-thinning and shear-thickening fluids behavior across the periodic array of cylinders. The above local features have been further explained in terms of global parameter (i.e. overall drag coefficients) as described below in the next section.

Further, the Fig. 2(b) shows the dependence of total drag coefficient (C_D) on the governing parameters; n, ϕ_s and Re. In Fig. 2(b), it can be seen that as the fluid behavior changes from shear-thinning to shear-thickening, the total drag coefficient increases with the solid volume fractions. This behavior is caused due to the varying the porosity of the cylinders. Further, the role of power-index also diminishes with the increasing value of solid volume fractions and thereby a shift in behavior of the shear-thinning and shear-thickening fluids takes place. These trends are consistent with the results of Soares et al. [12] and Spelt et al. [13].

B. Isotherm Profiles and Mean Nusselt Number (Nu)

Fig. 3(a) displays the isotherm patterns with the systematic variations of governing parameters; Re, Pr, n and ϕ_s . For a given ϕ_s , the gathering of isotherms in the flow domain is mounting with the increasing inertial effects. Further, the gathering of isotherms is more prominent when cylinders are closer to each other (ϕ_s = 0.30). At lower value of ϕ_s = 0.2.0, the upstream cylinder displays strongly sharper gradients in comparison to the downstream cylinder. Further, much steeper temperature gradients are seen nearer to the cylinders as Re increases. Certainly, this is because the heat transfer takes place mainly by the convection with the increasing values of Re. However, at the small Re (i. e. Re=1), the symmetrical isotherm patterns is seen which suggest that the conduction is dominating over convection. Further, the influence of power-law index (n) on the isotherm patterns are more insightful at higher Re. When the fluid nature shifts from shear-thickening to shear-thinning, a increasing density of isotherms tends to rise the temperature gradients. This happens because of the presence of the thinner thermal boundary layer in shear-thinning fluids as compared to corresponding Newtonian and/or shear-thickening fluids. These intricate local heat transfer feature has been further elaborated in terms of global behavior (i.e. mean Nusselt number) in the following section.

Further Fig. 3(b) shows the dependence of mean Nusselt number (Nu) on the governing parameters; Re, Pr, n and ϕ_s . It can be seen that as the n decreases, the Nusselt number increases and accordingly an improvement in the heat transfer has been noticed and specielly in the shear-thinning regions. Also, the Nusselt number diminishes with the increase in ϕ_s , which suggest that the resultant velocity and temperature gradients condense with a decrease in ϕ_s . The reverse patterns can be observed for the shear-thickening fluids. The increasing level of shear-thickening behavior decreases with increasing inertial effects.

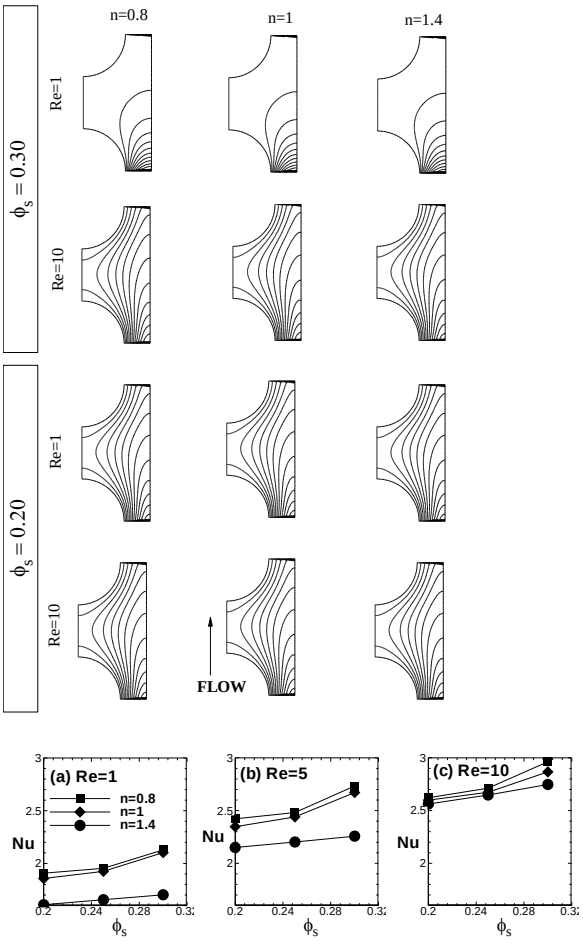

Fig. 3: (a) Isotherm profiles for ϕ_s = 0.20 and 0.30 and (b) Dependence of mean Nusselt number (Nu) on ϕ_s , Re and n

Additionally, the change in Nu is small at low Re as compared to high Re and it is concerned with the case when the heat transfer is mostly by conduction. In fact, a different kind of variations in the mean Nusselt number has been seen owing to shear-thinning and shear-thickening behaviors.

V. CONCLUSIONS

The steady flow of power-law fluids across periodic array of circular cylinders have been examined numerically using commercial CFD solver ANSYS-FLUENT. The local and global behavior have been explored with the variations of governing parameters (n, ϕ_f and Re and Pr). The drag coefficients were seen to increase with an increasing shear-thickening behavior and solid volume fractions. Irrespective of power-law index, as Re increases, the drag coefficient decreases correspondingly for all the solid volume fractions. Further, the maximum drags were observed when the cylinders were closer and thereafter, a corresponding decrease in drag coefficient was observed with solid volume fractions. Further, the thermal features were observed to be greatly influenced by the Re, Pr, n and ϕ_s . Particularly, shear-thinning behavior enhances the rate of heat transfer which further improves with increasing values of Re and ϕ_s along with the decreasing value of the n. In contrast, a reverse trend was observed for shear-thickening fluids under the alike situations. Overall, the flow and heat transfer parameters have shown to be strongly dependent over above governing parameters.

REFERENCES

[1] Sangani, A. S., Acrivos, A., 1982, Slow flow past periodic arrays of cylinders with application to heat transfer, Int. J. Multiphase Flow, 8, pp. 193- 206.

[2] Drummond, J. E., Tahir, M. I., 1984, Laminar viscous flow through regular arrays of parallel solid cylinders, Int. J. Multiphase Flow, 10, pp. 515- 540.

[3] Vijaysri, M., Chhabra R. P., Eswaran V., 1999, Power-law fluid flow across an array of in7nite circular cylinders: a numerical study, J. Non-Newt Fluid Mech., 87, pp. 263-282.

[4] Mandhani, V. K., Chhabra, R. P., Eswaran, V., 2002, Forced convection heat transfer in tube banks in cross flow, Chem. Eng. Sci., 57, pp. 379-391.

[5] Martin, A. R., Saltiel, C., Shyy, W., 1998, Frictional losses and convective heat transfer in sparse, periodic cylinder arrays in cross flow, Int. J. Heat Mass Transfer, 41, pp. 2383-2397.

[6] Koch, D. L., Ladd, A. J. C., 1997, Moderate Reynolds number flows through periodic and random arrays of aligned cylinders, J. Fluid Mech., 349, 31-66.

[7] Gamrat, G., Marinet, M. F., Stephane, L. P., 2008, Numerical study of heat transfer over banks of rods in small Reynolds number cross

flow, Int. J. Heat Mass Transfer, 51, pp. 853-864.

[8] Abrate, S., 2002, Resin flow in fiber preforms, Applied Mech. Reviews, 55, pp. 579-599.

[9] Ghosh, U. K., Upadhyay, S. N., 1994, Chhabra R P. Heat and mass transfer from immersed bodies to non-Newtonian fluids, Adv. Heat Transfer, 25, pp. 251-319.

[10] Chhabra, R. P., Richardson, J. F., 1999, Non-Newtonian Flow in the Process Industries, Butterwoth-Heinemann, Oxford, 1999.

[11] Chhabra, R P. 1999, In advances in the flow and Rheology of non-Newtonian fluids. Elsevier, Amsterdam, 1999; Chapter 39.

[12] Soares, A. A., Ferreira, J. M., Chhabra, R P., 2005, Flow and Forced Convection Heat Transfer in Crossflow of non-Newtonian fluids over a circular, Ind. Eng. Chem. Res., 44 pp. 5815-5827.

[13] Spelt, P. D. M., Selerland, T., Lawrence, C. J., Lee, P. D., 2005, Flow of inelastic Non-Newtonian fluids through arrays of aligned cylinders, Part II (Inertial effects for square arrays), J. Eng. Math., 51, pp. 81-97.

[14] Bruschke, M. V., Advani, S. G., 1993, Flow of generalized Newtonian fluids across a periodic array of cylinders, J. Rheo., 37, pp. 479-493.

[15] Mangadoddy, N. Bharti, R. P., Chhabra, R. P., Eswaran, V., 2004, Forced convection in cross flow of power-law fluids over a tube bank, Chem. Eng. Sci., 59, pp. 2213-2222.

[16] Bird, R. B., Stewart, W. E., Lightfoot, E. N., 2002, Transport Phenomena, 2nd Edition. Wiley, New York pp. 113).

[17] Bharti, R. P., Chhabra, R. P., Eswaran, V., 2007, Steady forced convection heat transfer from a heated circular cylinder to power-law fluids, Int. J. Heat Mass Transfer, 50, pp. 977-990.